Low-temperature water gas shift reaction on combustion synthesized $Ce_{1-x}Pt_xO_{2-\delta}$ catalyst

Parthasarathi Bera[a,**], Sachin Malwadkar[b], Arup Gayen[a], C.V.V. Satyanarayana[b], B.S. Rao[b], and M.S. Hegde[a,*]

[a]*Solid State and Structural Chemistry Unit, Indian Institute of Science, Bangalore 560012, India*
[b]*Catalysis Division, National Chemical Laboratory, Pune 411008, India*

Received 16 September 2003; accepted 30 April 2004

Catalytic activity of Pt^{2+} ion substituted CeO_2 synthesized by solution combustion method was tested for low-temperature water gas shift reaction in H_2 rich steam reformate. XPS studies show that Pt is dispersed as ions and there is no change in Pt oxidation state after the reaction. CO conversion is found to be maximum at 200 °C over $Ce_{1-x}Pt_xO_{2-\delta}$ catalysts without any methanation. The values of rate are 1.86 and 4.66 μmol/g/s at 125 and 150 °C respectively with a dry gas flow rate of 6 Lh^{-1} over 2% Pt/CeO_2.

KEY WORDS: combustion synthesis; $Ce_{1-x}Pt_xO_{2-\delta}$; low-temperature shift (LTS); H_2; fuel cell.

1. Introduction

The reaction of carbon monoxide with steam leading to carbon dioxide and hydrogen is generally called water gas shift (WGS) reaction and it is written as

$$CO + H_2O \rightleftharpoons H_2 + CO_2 \qquad (1)$$

It has been used as an important step in the industrial production of ammonia and hydrogen for many years [1,2]. Using this process, the CO levels of steam reformates can be brought down to below $<1\%$ and also valuable H_2 is extracted from water. This reaction is employed as a step to remove selectively traces of CO in presence of excess hydrogen in industry. During last 30 years many studies have been carried out towards designing new catalysts, kinetics and mechanism for WGS reaction [3–12]. Campbell *et al.* [4–6] have studied reaction kinetics for Cu based catalysts, whereas mechanism over MgO, ZnO, Rh/CeO_2 catalysts have been explored by Shido *et al.* [7–10]. Recently, Kochiloefl has reviewed several aspects of WGS reaction [13]. Two types of WGS catalysts that work in different temperature regions are widely used in industry. Iron/chromium oxide catalyst is found out to work in high temperature shift (HTS) reaction in the range of 320–450 °C, whereas $Cu/ZnO/Al_2O_3$ is used for the low-temperature shift (LTS) reaction between 150 and 250 °C. Gold dispersed on various supports such as Fe_2O_3, ZnO, TiO_2 and ZrO_2 have also been studied for LTS reaction [14–17].

At present, fuel cell technology is rapidly growing for both stationary and transportation applications [18]. In fuel cell, chemical energy of a fuel is directly converted into electrical energy without any thermal cycle. As a low emission, energy-efficient process, fuel cell may replace the internal combustion engine for automotive applications. Recently, WGS reaction has attracted much attention due to its potential use in fuel processors for production of H_2 by on-board steam reforming in PEM fuel cell [19,20]. Generally, reformate gas will contain H_2, CO, CO_2, H_2O and CH_4. CO is a pollutant and poisonous for noble metal catalysts in the electrodes of fuel cell. Therefore, advanced LTS catalysts are necessary to produce CO free hydrogen to feed fuel cell. In the last few years, ceria supported metal catalysts have been investigated for LTS reaction [21–25]. Flytzani-Stephanopoulos *et al.* have studied kinetics of WGS reaction over ceria supported Cu, Ni and Au catalysts [21,22].

Recently, solution combustion method has been found to be unique to obtain high surface area fine particles. This method involves rapid heating at 350 °C of an aqueous redox mixture containing stoichiometric amounts of corresponding metal nitrates and hydrazine based fuels [26,27]. The merits of the solution combustion technique are: (a) being a solution process, it has all the advantages of wet chemical process such as control of stoichiometry, doping of desired amount of impurity ions and forming nano size particles, (b) low-temperature initiated process, (c) highly exothermic due to redox reaction, (d) self propagating, (e) transient high temperature, (f) production of huge amount of gases, (g) formation of high surface area, voluminous and homogeneous product, (h) stabilization of metastable phases and (i) simple, fast and economical. In recent times, we have synthesized ceria supported metal catalyst by solution combustion method and studied their catalytic activities [28–30]. Here we report the investigation of

*To whom correspondence should be addressed.
E-mail: mshegde@sscu.iisc.ernet.in
**Present address: Department of Chemistry, University of Washington, Seattle, Washington 98195, USA.

1011-372X/04/0700–0213/0

low-temperature WGS reaction on $Ce_{1-x}Pt_xO_{2-\delta}$ catalyst prepared by solution combustion method. We show that WGS reaction occurs at low temperature over these catalysts in H_2 rich stream and $Ce_{1-x}Pt_xO_{2-\delta}$ ($x = 0.02$) exhibit good catalytic activity at high space velocities.

2. Experimental

2.1. Synthesis

The combustion mixture for the preparation of 1% Pt/CeO_2 contained $(NH_4)_2Ce(NO_3)_6$, H_2PtCl_6 and $C_2H_6N_4O_2$ (oxalyldihydrazide) in the mole ratio 0.99 : 0.01 : 2.38. Oxalyldihydrazide (ODH) prepared from diethyl oxalate and hydrazine hydrate was used as the fuel. In a typical preparation, 10 g of $(NH_4)_2Ce(NO_3)_6$ (E. Merck India Ltd., 99.9%), 0.095 g of H_2PtCl_6 (Ranbaxy Laboratories Ltd., 99%) and 5.175 g of ODH were dissolved in the minimum volume of water in a borosilicate dish of 130 cm^3 capacity. The dish containing the redox mixture was introduced into a muffle furnace maintained at 350 °C. Initially the solution boiled with frothing and foaming and underwent dehydration. At the point of complete dehydration, the surface ignited, burning with a flame (~1000 °C) and yielding a voluminous solid product within 2 min. These compounds were prepared in an open muffle furnace kept in a fume cupboard with exhaust. A similar procedure was followed for the preparation of 2% Pt/CeO_2 catalyst.

2.2. Characterization

XRD patterns of the as-prepared and spent catalyst were carried out with Rigaku-2000 diffractometer at a scan rate of 1° min^{-1} between 10 and 110 degrees. A JEOL JEM-200CX transmission electron microscope operated at 200 kV was used to carry out TEM studies.

XPS of these catalysts were recorded on an ESCA-3 Mark II spectrometer (VG Scientific Ltd., England) using AlK_α radiation (1486.6 eV). Binding energies were calculated with respect to C(1s) peak at 285 eV and measured with a precision of ±0.2 eV. XPS of spent catalyst was also carried out. For XPS analysis the powder samples were made into pellets of 8 mm diameter and placed into an ultrahigh vacuum (UHV) chamber at 10^{-9} Torr housing the analyzer. The experimental data were curve fitted with Gaussian peaks after subtracting a linear background.

2.3. Catalytic test

The experimental set up consists of two reactors. The first one is a steam reformer that supplies typical steam reformate feeds to the second WGS reactor containing the catalyst under investigation. Both the reactors are fixed bed down flow reactor operated in atmospheric pressure. A proprietary mixed oxide catalyst containing $NiO–CeO_2–ZrO_2$ was used for steam reforming of C_2H_5OH. The mixed oxide catalyst was reduced in hydrogen at 350 °C prior to the reaction. A feed consisting of C_2H_5OH and H_2O (1 : 8 molar ratio) was used as the input to the reformer. The reforming temperature was optimized (650 °C). The reformate (dry gas) at the outlet of steam reformer consists of H_2 (~71%), CO (~9%), CO_2 (~19%) and CH_4 (~1%), whereas wet gas contains 44% steam and 56% of dry gas that consists of above mentioned components. Hence, steam to dry gas ratio of the feed to WGS reactor is 0.79. A high precision syringe pump (ISCO Model 500D) was used to control and vary the liquid feed (C_2H_5OH and H_2O) to the steam reformer.

Output gas of the reformer along with the steam was fed to the second reactor (WGS reactor) that contains $Ce_{1-x}Pt_xO_{2-\delta}$ catalyst. The shift catalyst powder was pelleted and crushed to obtain particles in 20–30 mesh (600–850 μm in size) and these catalyst particles could not be catagorized into any specific shapes. About 8 g (3.5 cm^3 volume) of the catalyst was used without any dilution. Reaction temperature was measured at the outlet by a chromel–alumel thermocouple. Total input gas flow rate was in the range of 5–49 L h^{-1}. Accordingly, gas hourly space velocity (GHSV) was varied from 1400 to 14,000 h^{-1}. The reaction products were analyzed using an on-line gas chromatograph (Chemito Model 8610) equipped with a thermal conductivity detector, a gas sampling valve and Spherocarb packed (8 ft length and 1/8 in. diameter) column for separation of various gas components using argon as carrier.

3. Results and discussion

3.1. XRD studies

A detailed XRD study of 1% and 2% Pt/CeO_2 have been reported recently [29,30] where we have shown formation of solid solution of $Ce_{1-x}Pt_xO_{2-\delta}$ type with Pt largely in +2 state. Rietveld refinement is carried out for both 1 and 2% Pt/CeO_2 catalysts varying 19 parameters such as overall scale factor, background parameters, isotropic thermal parameters, unit cell, shape and oxygen occupancy. It has been observed that Pt^{2+} ion is substituted for Ce^{4+} ion in CeO_2 with oxide ion vacancy. A decrease in the lattice parameter $a = 5.4113$ (3) Å in pure CeO_2 to $a = 5.4105$ (2) Å in 1% Pt/CeO_2 has been observed. Oxygen content also decreased from 1.934 in pure CeO_2 to 1.883 in 1% Pt/CeO_2 indicating presence of more oxide ion vacancy. Lattice parameter a is 5.4106 (3) Å with oxygen occupancy of 1.921 for 2% Pt/CeO_2 catalyst. The increase in oxygen content in 2% Pt/CeO_2 compared to 1% Pt/CeO_2 could be due to the decrease in Pt^{2+} substitution into Ce^{4+} site since amount of Pt particles are higher in 2% Pt/CeO_2 in relation to 1% Pt/CeO_2 (see XPS studies). The Peaks due to PtO or PtO_2 could not be detected. All refined parameters of 1% and 2% Pt/CeO_2

Table 1
Rietveld refined parameters of Pt/CeO_2 catalysts along with CeO_2

Catalyst	a/Å	R_{Bragg} (%)	R_F (%)	R_P (%)	O_{occ}
CeO_2	5.4113 (3)	0.91	0.70	4.4	1.934
1% Pt/CeO_2	5.4105 (2)	1.31	0.819	3.4	1.883
2% Pt/CeO_2	5.4106 (3)	0.966	0.586	4.43	1.921

Lattice parameter – a.
Oxygen occupancy – O_{occ}.
Space group – Fm3m.
Profile function – Pseudo-Voigt.
Number of refined parameters – 19.

along with CeO_2 are shown in table 1. There is no change in XRD patterns of Pt/CeO_2 catalysts after WGS reaction.

3.2. TEM studies

Typical TEM image of as-prepared 2% Pt/CeO_2 is given in figure 1(a). The size of CeO_2 crystallites are in the range of 25–40 nm. The morphology of the crystallites is cubic. Further, Pt particles detectable in 2% Pt/CeO_2 are smaller in size (4–5 nm). TEM image shows that there are at least 1–2 particles of Pt^0 per each particle of CeO_2. Taking into account this, the mean size of Pt^0 is ~10 times less than for CeO_2 and that the molar volume of Pt (15.3 $Å^3$/Pt atom) is 2.58 times smaller than that of CeO_2 (39.6 $Å^3$/Ce atom). Therefore, the amount of Pt in the metallic particles is approximately 0.25–0.5% of the amount of Ce and metallic particles comprise 12–25% of Pt content. The polycrystalline electron diffraction ring pattern of 2% Pt/CeO_2 could be indexed to CeO_2 with fluorite structure. Thus, TEM studies demonstrate that over 2% Pt/CeO_2, small amount of Pt is present as metal particles and the rest are dispersed as atoms or ions which could not be detected. TEM image of 2% Pt/CeO_2 after WGS reaction is shown in figure 1(b). There is no significant change in the grain size of CeO_2 crystallites and density of Pt metal particles after the reaction.

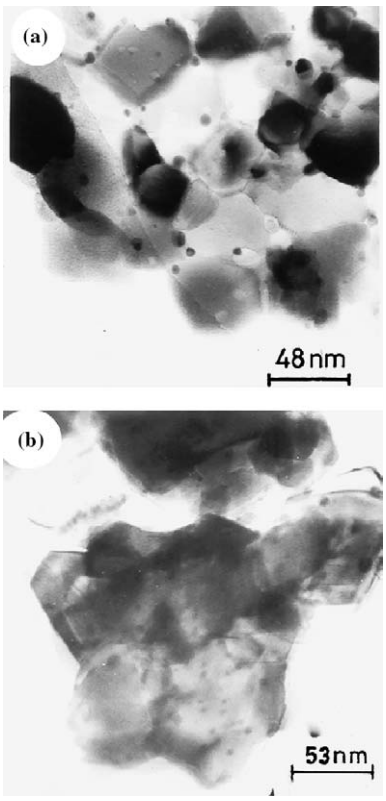

Figure 1. TEM images of 2% Pt/CeO_2: (a) as-prepared and (b) after WGS reaction.

3.3. XPS studies

XPS of Pt(4f) core level region in as-prepared 2% Pt/CeO_2 is given in figure 2. The spectra could be resolved into three sets of spin-orbit doublets. Accordingly, $Pt(4f_{7/2,\ 5/2})$ peaks at 71.0, 74.2; 72.0, 75.2 and 74.4, 77.6 eV could be assigned to Pt^0, Pt^{2+} and Pt^{4+} respectively [31,32]. Here Pt is found to be dispersed mostly in +2 (69%) and +4 (19%) oxidation states on CeO_2 crystallites with only 12% Pt present as Pt metal particles. This observation agrees well with the TEM studies. In the Pt(4f) spectra of the sample after the reaction slight decrease in the full width at half maximum (FWHM) of different Pt(4f) species is observed. However, no increase in the Pt^0 component is seen. Similarly, XPS of Pt(4f) core level region of 1% Pt/CeO_2 also shows peaks corresponding to Pt^0 (7%), Pt^{2+} (72%) and Pt^{4+} (21%).

Ce(3d) core level peaks obtained from XPS of as-prepared 2% Pt/CeO_2 sample are given in figure 3. $Ce(3d_{5/2,\ 3/2})$ peaks at 882.9 and 901.3 eV with characteristic satellites (marked in the figure) correspond to

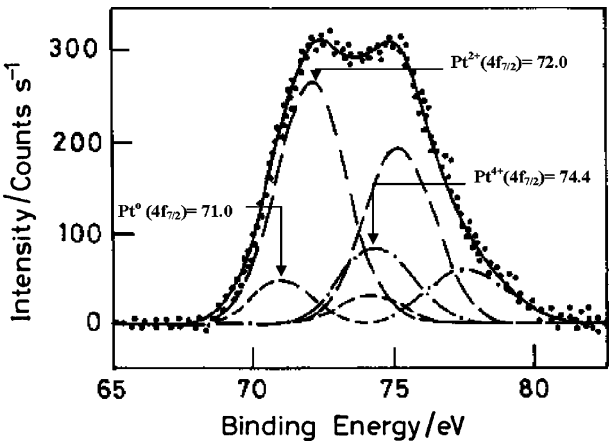

Figure 2. XPS of core level region of Pt(4f) in as-prepared 2% Pt/CeO_2 catalyst.

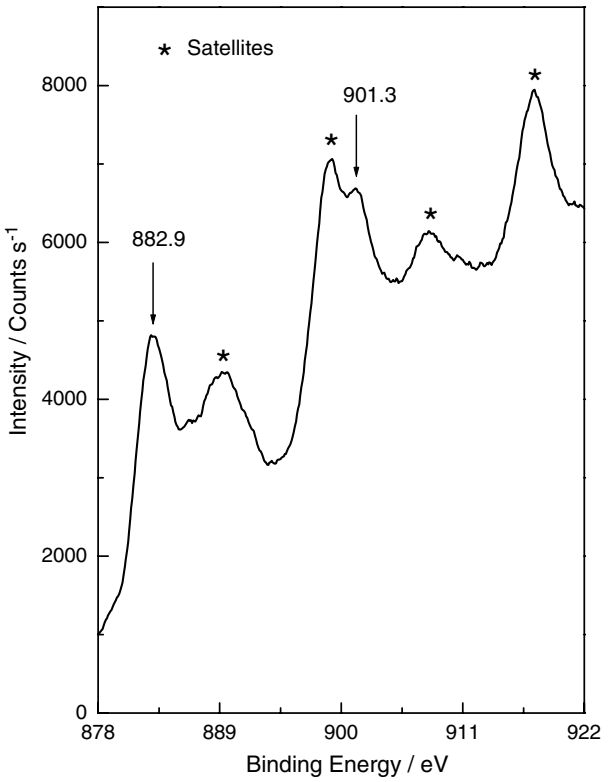

Figure 3. XPS of core level region of Ce(3d) in as-prepared 2% Pt/CeO_2 catalyst.

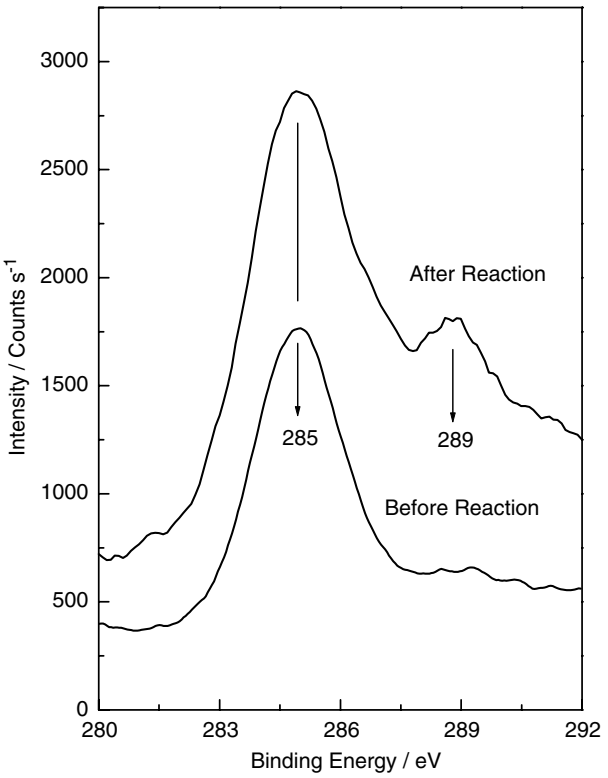

Figure 4. XPS of core level region of C(1s) in 2% Pt/CeO_2: before and after WGS reaction.

CeO_2 with Ce in +4 oxidation state [31,33]. Intensity and positions of Ce(3d) peaks remain the same after the WGS reaction. No reduction of Ce^{4+} to Ce^{3+} is observed in the XPS of the catalyst after the reaction.

In figure 4, C(1s) spectra in 2% Pt/CeO_2 before and after WGS reaction are shown. C(1s) peak is observed at 285 eV and there is no significant change in the peak position in the spent catalyst. A small peak at 289 eV may be due to surface carbonate formation. Further, total intensity of C(1s) as well as C(1s) to Ce(3d) integrated intensity ratio are slightly increased in the sample after the reaction due to surface carbonate formation.

The surface concentration of Pt in Pt/CeO_2 is estimated by the relation:

$$\frac{X_{Pt}}{X_{Ce}} = \frac{I_{Pt}\sigma_{Ce}\lambda_{Ce}D_E(Ce)}{I_{Ce}\sigma_{Pt}\lambda_{Pt}D_E(Pt)} \quad (2)$$

where X, I, σ, λ, and D_E are the surface concentration, intensity, photoionization cross section, mean escape depth and geometric factor respectively. Integrated intensities of Pt(4f) and Ce(3d) core level peaks have been taken into account to estimate the concentration. Photoionization cross sections and mean escape depths have been obtained from the literature [34,35]. Accordingly, surface concentration of Pt in as-prepared 2% Pt/CeO_2 is 20% and there is no decrease in the surface concentration of Pt after the reaction.

3.4. Catalytic studies

WGS reaction was carried out over 1% and 2% Pt/CeO_2 catalysts using CO containing H_2 rich steam reformate exiting the C_2H_5OH reformer. The CO conversion profiles in WGS reaction over 1% and 2% Pt/CeO_2 catalysts as a function of temperature are shown in figure 5. From the figure it is clear that up to 90% of CO is converted at 200 °C over 2% Pt/CeO_2. Due to WGS reaction CO was converted to CO_2 up to 200 °C over these catalysts and additional H_2 was produced without any methanation up to this temper-

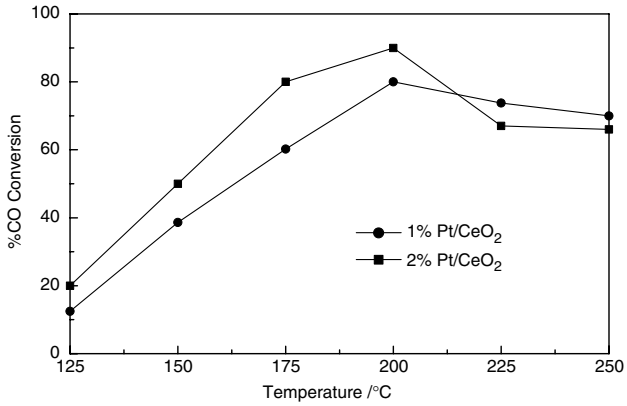

Figure 5. %CO conversion in WGS reaction over 1% and 2% Pt/CeO_2 as a function of temperature at a GHSV of 2600 h^{-1}.

ature. But at higher temperature (>225 °C) CH_4 formation was observed due to reaction among CO, CO_2 and H_2. Similarly, reverse WGS reaction could not be ruled out at higher temperature. Sekizawa *et al.* observed reverse WGS reaction over $Cu/ZnO/Al_2O_3$ catalyst at low CO concentration (0.6 vol% CO) in the input gas [36]. Therefore, all these non selective reactions led to a small reduction in H_2 concentration in the product gas stream. The catalytic activity on combustion synthesized Pt/CeO_2 catalysts employed in the present study is higher than that on supported gold catalysts like Au/Fe_2O_3, Au/ZrO_2 and Au/ZnO reported by Andreeva's group [15,17]. About 90% CO conversion is observed over 2% Au/Fe_2O_3 at 360 °C at a GHSV 4000 h^{-1} with 4.88 vol% CO in the input gas, whereas 90% CO conversion occurs over Au/Fe_2O_3 and Au/ZrO_2 at 300 °C at a GHSV 4000 h^{-1} with 4.03 vol% CO in the input gas. WGS reaction occurs above 300 °C over noble metals (Pt, Pd and Rh) supported CeO_2 catalysts supplied by Johnson Matthey at a GHSV of 16,000 h^{-1} [37]. Pt/CeO_2 catalyst prepared by hydrothermal method shows WGS activity above 250 °C where input dry gas contains 10 vol% CO [38]. About 65% CO conversion is observed over this catalyst at 350 °C. About 80% CO conversion occurs at 325 °C over several Pt/CeO_2 catalysts prepared by coprecipitation, homogeneous precipitation and decomposition methods with 1.5 vol% CO in the input dry gas [25].

WGS reaction is an equilibrium controlled chemical reaction [2] and therefore reaction equilibrium constant (K_p) for WGS reaction over 2% Pt/CeO_2 catalyst is calculated and compared with the literature data. At 200 °C, K_p value is estimated to be 27.3 (calculated by dividing the concentration of products, CO_2 and H_2 by concentration of reactants, CO and H_2O) and this value matches for the K_p at 326 °C from the literature [39]. This indicates that reaction is 126 °C away from the equilibrium. We have used feeds that contain high concentration of steam and hence K_p is expected to be lower under this condition. If the catalyst would have brought the outlet gas mixture to its equilibrium, CO concentration would have been close to 0.13% (calculated by using K_p value of 210.8 at 200 °C [39]) in the dry gas instead of 0.92%.

Water gas shift reaction was also carried out at different GHSV. Figure 6 shows %CO conversion over 1 and 2% Pt/CeO_2 as a function of GHSV at 200 °C. CO conversion is as high as 88% at 1400 h^{-1} GHSV over 1% Pt/CeO_2 and some decay in catalytic activity is observed when GHSV is raised upto 14,000 h^{-1}. On the other hand, on 2% Pt/CeO_2, low CO concentration is observed at a GHSV of 1400 h^{-1}, while it increases to 88% at a GHSV of 3000 h^{-1} and remains steady (above 80%) even at higher GHSVs (upto 14,000 h^{-1}). Therefore, 2% Pt/CeO_2 shows better activity than 1% Pt/CeO_2 at higher GHSV. Also there is no deactivation of catalyst after the prolonged reaction. Considering that

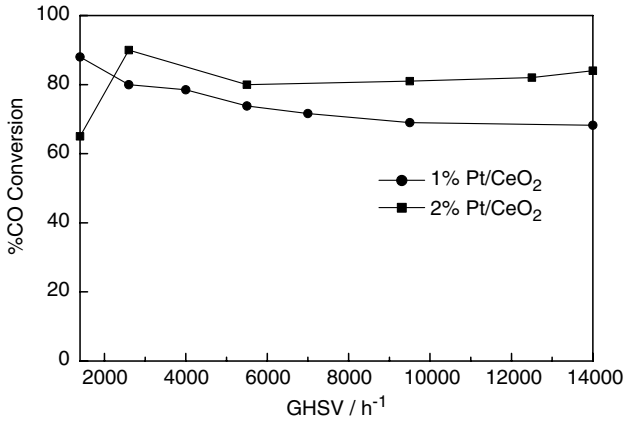

Figure 6. %CO conversion in WGS reaction over 1% and 2% Pt/CeO_2 as a function of GHSV at 200 °C.

commercial catalysts available at present can not handle high GHSVs, this finding has an important bearing on the developmental efforts on the low-temperature WGS catalysts at high GHSV.

The reaction rate of the WGS reaction is calculated by the equation [40]

$$\text{Rate} = \frac{FX}{vW} \tag{3}$$

where F = inlet molar dry gas flow rate, X = fractional CO conversion at a particular temperature, v = stoichiometric coefficient of CO and W = weight of the catalyst. The rate is expressed in μmol/g/s. The rates of the WGS reaction over Pt/CeO_2 catalysts at different temperatures are given in table 2. The rate over combustion synthesized 2% Pt/CeO_2 at 200 °C is 8.39 μmol/g/s which could be comparable with WGS reaction rate of 7.6 μmol/g/s over commercial 40% $CuO/ZnO/Al_2O_3$ catalyst supplied by United Catalysts [41]. The turnover frequencies (TOF) of WGS reaction at low CO conversions have been obtained after dividing the reaction rate by active site concentration. Here surface Pt^{2+} concentration as calculated by XPS was considered for the calculation of TOF. TOF is expressed in s^{-1}. TOFs are 0.013 and 0.025 s^{-1} at 100 and 125 °C respectively over 1% Pt/CeO_2, whereas these are 0.005 and 0.02 s^{-1} at the same temperatures over 2% Pt/CeO_2. It is important to

Table 2
Rate (μmol g^{-1} s^{-1}) of WGS reaction over 1% and 2% Pt/CeO_2 catalysts at different temperatures at a dry gas flow rate of 6 L h^{-1}

Temperature (°C)	1% Pt/CeO_2	2% Pt/CeO_2
100	0.64	0.38
125	1.20	1.86
150	3.60	4.66
175	5.61	7.46
200	7.46	8.39
225	6.88	6.25
250	6.52	6.15

note that rate continues to increase even up to GHSV 14,000 h^{-1}. If we calculate reaction rate using molar flow rate of CO with respect to Pt amount present in the catalyst, then reaction rate would be 8.25×10^{-5} and 7.61×10^{-5} mol CO g_{Pt}^{-1} s^{-1} at 200 and 225 °C over 1%Pt/CeO_2 respectively. Similarly, rate would be 4.9×10^{-5} and 3.6×10^{-5} mol CO g_{Pt}^{-1} s^{-1} at 200 and 225 °C over 2%Pt/CeO_2 respectively. The WGS reaction rate over $Cu/ZnO/Al_2O_3$ catalyst [42] at 230 °C is 1.53×10^{-4} mol CO g_{Cu}^{-1} s^{-1} which is ~2 times higher than 7.61×10^{-5} mol CO g_{Pt}^{-1} s^{-1} at 225 °C over 1% Pt/CeO_2. About 80% CO conversion occurs over 30% $Cu/ZnO/Al_2O_3$ catalyst at 200 °C with a GHSV 7200 h^{-1} [36]. 80% CO conversion is observed over Cu/MnO catalyst at 225 °C with a GHSV 6400 h^{-1}, whereas 75% CO conversion occurs at 200 °C over $Cu/ZnO/Al_2O_3$ catalyst with same GHSV [43]. About 90% CO conversion occurs over impregnated 5% $Cu/ZnO/Al_2O_3$ catalyst with a GHSV 6400 h^{-1} which is comparable to that prepared by conventional coprecipated method [44]. Recently, Luengnaruemitchai *et al.* have reported low-temperature WGS reaction over sol-gel prepared 1% Pt/CeO_2 [45]. Although the space velocity they employed is higher than that used in the present study, but the temperature of maximum CO conversion is more than 250 °C with 0.5 vol% CO in the feed which decreases rapidly on increasing the CO concentration. Also the WGS activity is low in presence of excess hydrogen. Thus, the combustion synthesized $Ce_{1-x}Pt_xO_{2-\delta}$ catalyst reported here shows high WGS activity at low-temperature under hydrogen rich condition and high CO concentration (~10 vol%) in the dry gas. Hence, only one catalyst, instead of a combination of HTS and LTS in sequence can handle the WGS requirements of a fuel processor thus leading to its reduction in size.

The present study is an attempt to obtain highly active and more stable catalysts for WGS reaction. The combustion method produces Pt/CeO_2 nano crystallites of 30–40 nm. XPS studies of 2% Pt/CeO_2 show that Pt is dispersed mostly in +2 (69%) and +4 (19%) oxidation states on CeO_2 crystallites with about 12% Pt in the Pt^0 state. It has been demonstrated that there is a Pt^{2+} ion–ceria interaction that leads to the formation of solid solution, $Ce_{1-x}Pt_xO_{2-\delta}$ on the CeO_2 surface having $-Pt^{2+}-O-Ce^{4+}-$ linkages [29]. Here, Pt^{2+} ions are substituted into Ce^{4+} sites in CeO_2 matrix creating oxide ion vacancy. XPS analysis of the catalyst shows that there is no change in concentration of different oxidation states of Pt after the reaction. There is a little increase in the carbon content over the catalyst after the reaction as shown from XPS. Therefore, the catalyst is stable at the reaction condition. We believe that presence of excess H_2O even in the presence of excess H_2 is responsible for keeping the Pt in oxidized state in the $Ce_{1-x}Pt_xO_{2-\delta}$. That Pt^{2+} ion is the active site for CO adsorption has been shown earlier [28]. For WGS reaction the oxygen from H_2O needs to be extracted. One possible way is that oxygen vacancy created in CeO_2 due to the Pt^{2+} ion substitution may act as the active site for H_2O adsorption via oxygen. Abstraction of oxygen by CO forming a more stable CO_2 molecule would lead to release of H_2.

4. Conclusions

The salient features of this investigation are:

(1) Platinum is stabilized mainly in +2 oxidation state on nanosized CeO_2 in the form of $Ce_{1-x}Pt_xO_{2-\delta}$ phase.
(2) Platinum ions are active sites in $Ce_{1-x}Pt_xO_{2-\delta}$ catalysts for low-temperature WGS reaction with high CO conversion.
(3) Pt ion substituted CeO_2 catalysts show high rates for WGS reaction.
(4) Equilibrium concentration of CO for WGS reaction over 2% Pt/CeO_2 is 0.13% in the dry gas at 200 °C.
(5) Since the catalyst reported here can handle high CO concentrations as input and bring it down to reasonably low levels (< 1 vol%), it has the potential to replace the present HTS and LTS combination in fuel processor which is used in sequence. This may have substantial gain in terms of reduction in the processor size.

Acknowledgments

A. Gayen is thankful to Council of Scientific and Industrial Research (CSIR), Government of India for the award of a research fellowship. Financial support from the Department of Science and Technology (DST), Government of India is gratefully acknowledged.

References

[1] L. Lloyd, D.E. Ridler and M.V. Twigg, in: *Catalyst Handbook*, 2nd ed., ed. M.V. Twigg (Wolfe Publishing Ltd, London, 1989), ch. 6, p. 283.
[2] D.S. Newsome, Catal. Rev. Sci. Eng. 21 (1980) 275.
[3] L. Mendelovici and M. Steinberg, J. Catal. 96 (1985) 285.
[4] C.T. Campbell and K.A. Daube, J. Catal. 104 (1987) 109.
[5] J. Nakamura, J.M. Campbell and C.T. Campbell, J. Chem. Soc., Faraday Trans. 86 (1990) 2725.
[6] C.V. Ovesen, P. Stoltze, J.K. Nørskov and C.T. Campbell, J. Catal. 134 (1992) 445.
[7] T. Shido, K. Asakura and Y. Iwasawa, J. Catal. 122 (1990) 55.
[8] T. Shido and Y. Iwasawa, J. Catal. 129 (1991) 343.
[9] T. Shido and Y. Iwasawa, J. Catal. 136 (1992) 493.
[10] T. Shido and Y. Iwasawa, J. Catal. 141 (1993) 71.
[11] C. Rhodes, G.J. Hutching and A.M. Ward, Catal. Today 23 (1995) 43.
[12] C.V. Ovesen, B.S. Clausen, B.S. Hammershøi, G. Steffensen, T. Askgaard, I. Chorkendorff, J.K. Nørskov, P.B. Rasmussen, P. Stoltze and P. Taylor, J. Catal. 158 (1996) 170.

[13] K. Kochloefl, in: *Handbook of Heterogeneous Catalysis*, Vol. 1, eds. G. Ertl, H. Knözinger and J. Weitkamp (VCH, Weinheim, 1997) p. 1831.
[14] D. Andreeva, V. Idakiev, T. Tabakova and A. Andreev, J. Catal. 158 (1996) 354.
[15] D. Andreeva, V. Idakiev, T. Tabakova, A. Andreev and R. Giovanoli, Appl. Catal. A 134 (1996) 275.
[16] F. Boccuzzi, A. Chiorino, M. Manzoli, D. Andreeva and T. Tabakova, J. Catal. 188 (1999) 176.
[17] T. Tabakova, V. Idakiev, D. Andreeva and I. Mitov, Appl. Catal. A 202 (2000) 91.
[18] J.R. Rostrup-Nielsen, Phys. Chem. Chem. Phys. 3 (2001) 283.
[19] S. Ahmed and M. Krumpelt, Int. J. Hydrogen Energy 26 (2001) 291.
[20] L.F. Brown, Int. J. Hydrogen Energy 26 (2001) 381.
[21] Y. Li, Q. Fu and M. Flytzani-Stephanopoulos, Appl. Catal. B 27 (2000) 179.
[22] Q. Fu, A. Weber and M. Flytzani-Stephanopoulos, Catal. Lett. 77 (2001) 87.
[23] T. Bunluesin, R.J. Gorte and G.W. Graham, Appl. Catal. B 15 (1998) 107.
[24] S. Hilaire, X. Wang, T. Luo, R.J. Gorte and J. Wagner, Appl. Catal. A 215 (2001) 271.
[25] G. Jacobs, L. Williams, U. Graham, G.A. Thomas, D.E. Sparks and B.H. Davis, Appl. Catal. A 252 (2003) 107.
[26] K.C. Patil, S.T. Aruna and S. Ekambaram, Curr. Opin. Solid State Mater. Sci. 2 (1997) 158.
[27] K.C. Patil, S.T. Aruna and T. Mimani, Curr. Opin. Solid State Mater. Sci. 6 (2002) 507.
[28] P. Bera, K.C. Patil, V. Jayaram, G.N. Subbanna and M.S. Hegde, J. Catal. 196 (2000) 293.
[29] P. Bera, K.R. Priolkar, A. Gayen, P.R. Sarode, M.S. Hegde, S. Emura, R. Kumashiro, V. Jayaram and G.N. Subbanna, Chem. Mater. 15 (2003) 2049.
[30] P. Bera, A. Gayen, M.S. Hegde, N.P. Lalla, L. Spadaro, F. Frusteri and F. Arena, J. Phys. Chem. B 107 (2003) 6122.
[31] T. Jin, Y. Zhou, G.J. Mains and J.M. White, J. Phys. Chem. 91 (1987) 5931.
[32] J.Z. Shyu and K. Otto, J. Catal. 115 (1989) 16.
[33] D.D. Sarma, M.S. Hegde and C.N.R. Rao, J. Chem. Soc., Faraday Trans. 277 (1981) 1509.
[34] J.H. Scofield, J. Electron Spectrosc. Relat. Phenom. 8 (1976) 129.
[35] D.R. Penn, J. Electron Spectrosc. Relat. Phenom. 9 (1976) 29.
[36] K. Sekizawa, S. Yano, K. Eguchi and H. Arai, Appl. Catal. A, 169 (1998) 291.
[37] B.I. Whittington, C.J. Jiang and D.L. Trimm, Catal. Today 26 (1995) 41.
[38] S.L. Swartz, M. M. Seabaugh, C.T. Holt and W.J. Dawson, Fuel Cells Bull. 4 (2001) 7.
[39] M.V. Twigg, in: *Catalyst Handbook*, 2nd ed. (Wolfe Publishing Ltd, London, 1989) Appendix 7, p. 543.
[40] R.L. Burwell Jr., Pure Appl. Chem. 46 (1976) 71.
[41] N.A. Koryabkina, A.A. Pathak, W.F. Ruettinger, R.J. Farrauto and F.H. Ribeiro, J. Catal. 217 (2003) 233.
[42] M.J.L. Ginés, N. Amadeo, M. Laborde and C.R. Apesteguía, Appl. Catal. A 131 (1995) 283.
[43] Y. Tanaka, T. Utaka, R. Kikuchi, T. Takeguchi, K. Sasaki and K. Eguchi, J. Catal. 215 (2003) 271.
[44] Y. Tanaka, T. Utaka, R. Kikuchi, K. Sasaki and E. Eguchi, Appl. Catal. A 238 (2003) 11.
[45] A. Luengnaruemitchai, S. Osuwan and E. Gulari, Catal. Commun. 4 (2003) 215.